Anti-corrosion coating for metal surfaces based on superhydrophobic electrosprayed carbon layers

Julio J. Conde, Paloma Ferreira-Aparicio, Antonio M. Chaparro
Dep. of Energy, CIEMAT. Av. Complutense 40, 28040 Madrid (Spain)
Tel.: +34-913462607
Fax: +34-913466604
juliojose.conde@ciemat.es

Abstract

The electrospray deposition of a carbon-polymer ink has been used for the preparation corrosion protective coatings for metal substrates. The electrosprayed carbon layers are adherent and have highly porous structure that renders Cassie-Baxter type superhydrophobicity. The analysis of their morphology with SEM shows changes in the shape of aggregates with thickness that slightly affects their interaction with water and superhydrophobicity, as a consequence of changing electrospray deposition conditions. Stainless steel immersed in acidic aqueous solutions is efficiently protected from chemical and electrochemical corrosion when coated with electrosprayed carbon layers. The carbon layers with loads above 0.4 $mg \cdot cm^{-2}$ are able to avoid water contact with the metallic surface, permanently and during electrochemical polarization, thanks to their internal superhydrophobicity. Electrosprayed carbon coatings convey cheap and durable protection against aqueous corrosive environments. This coating procedure is very appropriate for the durability of internal components in fuel cells (plates, contacts), electrolyzers, and batteries working with aqueous solutions, due to its superhydrophobicity and good conductivity that provide stable electronic contact and fast water transport.

1. Introduction

The development of protective coatings for metallic surfaces is an issue of major interest for the reliability and durability of many electrochemical devices working in aqueous media, like the proton exchange membrane fuel cells (PEMFCs). The highest performance in PEMFCs can be obtained when the membrane is optimally humidified while avoiding the flooding of the electrodes, which requires optimal water management and an appropriate water rejection. In a standard configuration, generated water drops arriving at the back of the electrodes enter a grooved plate (flow field plate) where they are efficiently dragged by a gas stream towards the outlet. The flow field plate also collects the electronic current generated, so it must be of a highly conductive material. The important tasks performed by flow field plates (collecting current, separating the individual cells, distributing fuel and oxidant, carrying water out of each cell, and, in some cases, cooling the cells) is properly achieved by using stainless steel plates due to their high strength, no brittleness, no permeability to reactant gases, and especially the possibility for low-cost mass production [1]. However, their surface must be properly coated to avoid dissolution and growth of oxides, causing loss of conductivity, and ions that may contaminate other components like the catalyst and the membrane electrolyte. At the same time, the coating should improve water transport to the ambient. Coatings with high hydrophobicity and conductivity are most appropriate to accomplish with these requirements. Good electronic conductivity, fast water transport, and good (electro-)chemical stability are mandatory, therefore, for the cell contact.

Carbon-polymer composite coatings have been already studied for bipolar plate protection of PEMFC, but the substrates were found to not be sufficiently protected from the electrolyte due to the high porosity of the layer [2]. Surface hydrophobization has been widely used as a solution for corrosion protection [3,4] and self-cleaning [5] of metallic substrates. Since superhydrophobic surfaces have been proven to prevent water infiltration into porous films

[6] and thus limiting the exposure of corrosive media to the protected metallic surface [7], electrosprayed carbon might be an ideal candidate to fulfill all the requirements as a coating layer for the internal metallic components of PEMFC, by combining good electronic conductivity with high macroporosity, and hydrophobicity [8].

In recent years, our group has used electrosprayed films of Pt/C and Nafion as catalyst layers showing superior water transport capability and stability, with improved cell efficiencies, above 20% with respect to standard layers [8], and durability [9]. In a recent study, physico-chemical properties of carbon layers prepared by electrospray in the presence of Nafion ionomer/binder were investigated [10]. A strong and stable interaction between the sulfonic groups of the Nafion and the carbon surface was concluded, that favors close coverage of the carbon surface by the polymer chains. Fluorocarbon backbones appear to be oriented towards the outer part of the aggregates. Such special chemistry of the surface of carbon aggregates resulting from the electrospray deposition in the presence of Nafion contributes to shape the morphology and internal superhydrophobicity of the layers.

In this work, the electrospray deposition of carbon layers on stainless steel metallic surfaces is carried out to study their protective behavior in strong acidic media. With this aim, carbon layers have been deposited with variable thickness. Conventional airbrushing was used as a control method for deposition of carbon porous layers with the same loading and composition. The resulting electrosprayed films are shown to be structurally stable and provide a protective coating for metals against corrosion, in contrast with those prepared by airbrushing.

2. Experiments

Carbon black-ionomer (20 wt%) composite films were prepared from inks of carbon black (Vulcan XC 72R, Cabot, S(BET) = 230 $m^2 \cdot g^{-1}$), Nafion® perfluorinated ion exchange resin (5

wt% in lower aliphatic alcohols and water, Aldrich), and isopropanol (Panreac), with 1% solid content. The metal substrate was a 1.5 x 0.1 cm stainless steel (SS-310S) disk. Previous to deposition, the substrate was polished with grinding paper (Buehler Grit 180), and washed in sonicated ethanol-acetone solution. Electrospray was carried out using the set-up described in previous works [8], by applying 7.5-8 kV, with 2.5-3.0 cm needle-to-substrate distance, and 0.20-0.40 $mL \cdot h^{-1}$ ink flow rate. During deposition, substrate temperature was kept at 50 ºC, and ink temperature at 22 ºC under ultrasonic stirring. Hydrophobicity of the carbon layers was tested by means of water contact angle measurements, using an optical tensiometer (Theta 200 Basic, Biolin Scientific) at ambient temperature (23 °C) and relative humidity (30−35%). The angle measurements were taken after 400 s water drop contact. Before the hydrophobicity measurements, a 'hydrophilic treatment' was carried out on the films, consisting in the immersion in H_2SO_4 0.5M for at least 24 h, in order to stabilize their interaction with water. SEM images of the films surface were obtained by scanning electron microscopy (Hitachi FE-SEM SU-6600) using a secondary electron detector and accelerating voltage of 10 kV. The thickness of the layers was determined from these images. Optical images of the substrate surface before and after corrosion were taken with a Leica DM4M microscope.

Protective character of the carbon layers on the substrate was tested using electrochemical methods. Cyclic voltammetry and chronoamperometric experiments were performed using a commercial three electrode cell (Radiometer Analytical, Model C145/170), with the carbon coated disk as working electrode, using a sample holder that adjust the exposed geometric area to 1 cm^2, and a platinum counter electrode. A homemade mercury-mercurous sulfate (Hg/Hg_2SO_4, 1M H_2SO_4) was used as reference electrode, with a potential of 619 mV vs. SHE at 20 ºC [11]. Additionally, linear sweep voltammetry tests were performed in order to estimate the corrosion potential and the corrosion current density using the Tafel slope

extrapolation method and the Stern-Geary method. The electrolyte was H_2SO_4 0.5M at ambient temperature (21 ºC), deaerated by bubbling N_2 for ½ h before measurements, and cell blanketing with the same gas during measurements.

3. Results and discussion

3.1 Morphology and surface hydrophobicity of carbon layers

The surface of the porous carbon layers deposited on flat metallic plates is shown in SEM images of Fig. 1. The electrospray deposited films (Fig. 1a) are highly macroporous with pores of micrometric size.

A closer view of the morphology of electrosprayed layers is presented in Fig. 2, where three films with increasing carbon loads are shown. A groove made on the films reveals changes in the morphology of the coating with depth. For the observation of the cross-sectional profile, the angle of the sample in SEM was set to 40º, with respect to the perpendicular plane of the electron beam.

At the lowest carbon loading, 0.17 $mg \cdot cm^{-2}$ (Fig. 2-ES1), the layer shows a morphology with small agglomerates (typically below 10μm) and submicrometer dendritic growths can be distinguished; on increasing the load, the growth morphology changes to larger globular agglomerates (>20-30 μm) growing on top of the initial ones (Fig. 2-ES2 and 2-ES3). The modification in morphology and size of agglomerates reflect changing conditions for the electrospray film growth process. The initial dendritic shapes may reflect a growth governed by electric field induced transport of the particles over the film surface [12]; by increasing film thickness, the evolution to more globular growth reflect a change with predominance of particle-particle interactions over electrostatic forces. A probable cause for this change is the relaxation of electrostatic forces by the dielectric properties of the growing film.

The film thickness estimated from SEM profiles is plotted in Fig. 3 as a function of the carbon load in the coating. Determining a precise value for electrosprayed layers is not possible here due to the rough profile shown in Fig.2. However, an evolution of an average thickness can be inferred, showing initially low dependence, approximately below 0.2 $mg_C \cdot cm^{-2}$, followed by a period of larger thickness increase with carbon load, 17.6 $cm^3 \cdot g_C^{-1}$ in the 0.2-0.6 $mg_C \cdot cm^{-2}$. Such change obviously corresponds to the morphology change from dendritic to globular shape observed with SEM images (cf. Fig. 2). In contrast, the airbrushed film shows a constant thickness dependence on carbon concentration (3.3 $cm^3 \cdot g_C^{-1}$). A density of 0.30 $g \cdot cm^{-3}$ can be determined for these latter films, only slightly superior to the nominal density of Vulcan XC72R (0.264 $g \cdot cm^{-3}$). At the highest amount of carbon coating (0.8 $mg_C \cdot cm^{-2}$), the thickness of the electrosprayed film is almost 4 times larger than that of the airbrushed film.

The surface hydrophobicity of the layers was studied by the water contact angle technique. Measurements were carried out on freshly prepared films, before and after immersion in H_2SO_4 0.5M for 24 h in order to analyze the stability of their surface after interaction with an aqueous medium. Results are shown in Fig. 4. On the airbrushed films, such hydrophilic treatment gives rise to an important change in the water contact angle, from $\Theta > 150^o$ for the as-grown layer to $\Theta < 100^o$ after its immersion; in contrast, no significant change after hydrophilic treatment was observed for electrosprayed films, reflecting a durable and stable superhydrophobic character ($\Theta > 150^o$). Superhydrophobicity is reflected by many other observations. Upon immersion in liquid, a permanent air cushion on top of the electrosprayed layer was observed, allowing minimal contact of the electrolyte with the surface of the carbon composite layer. This effect was also observed in other types of superhydrophobic surfaces

[13, 14]. Also, water drops falling onto the surface of the layer do not stick on it and are instantly ejected, reflecting its superhydrophobicity (see video 1 in supplementary material).

The contact angle measurements in Fig. 4 show a clear dependence of hydrophobicity of electrosprayed films with carbon load that can be related to the change in the morphology of the layer, from dendritic to globular (cf. Fig. 2). The initial dendritic morphology is characterized by the highest superhydrophobicity (Θ > 168º), whereas the globular morphology gives rise to some decrease (Θ = 163º). The airbrushed layer shows less hydrophobic character with contact angle values below 100º and decreasing steadily with film thickness.

Since chemical modification may increase hydrophobicity to contact angles of up to 120°, but not more, superhydrophobicity must be a main consequence of the surface morphology, the so-called Lotus' effect, when roughness patterns are below the capillary length [15]. Roughness could also increase wettability if the interaction of water with the surface is energetically favored. Both cases have been explained by the well-known Wenzel model (increase hydrophilicity) and Cassie-Baxter model (increase hydrophobicity), leading, respectively, to the following relations between the observed contact angle, Θ, and the Young's contact angle of a flat surface, Θ_0:

$$\cos\theta = R_f \cos\theta_0 \quad (1)$$

$$\cos\theta = -1 + (1 - \cos\theta_0)\, f \quad (2)$$

Where R_f is the roughness factor in the Wenzel expression (Eq. 1), and f is the area fraction of the wetted part of the solid in the Cassie-Baxter expression (Eq. 2). The Wenzel and Cassie-Baxter relations (1) and (2) have classically been used to characterize the apparent contact

angles with remarkable success. The latter reveals that θ comes near 180° as f approaches to zero. Wetting in the Cassie-Baxter's state, rather than in the Wenzel state is a requirement for achieving superhydrophobicity. For the carbon films studied here, having identical chemical composition but different morphology, the water contact angle with the flat surface could be considered close to that obtained for the thickest aerography layer ($\theta_0 \approx 85°$). The superhydrophobicity of electrosprayed films corresponds to very low values of f (1-2% and 4-5% below and above 0.4 $mg \cdot cm^{-2}$, respectively), which could only be attained by a dendritic morphology resulting from the deposition process. The resulting distribution and orientation of the Nafion chains across the surface of the carbon after the electrospray process, reported in previous work, may contribute to the superhydrophobicity [10].

3.2 Electrochemical characterization and bulk film hydrophobicity

Stainless steel substrates coated with carbon black were studied in contact with 0.5M H_2SO_4 solution. Fig. 5 shows the voltammetric response of electrosprayed (Fig. 5a and 5b) and airbrushed (Fig. 5c) coatings with different carbon loads. The shape of the curves resembles carbon material voltammetries, including curve tilting and small peaks in the limits of the potential window due to pseudocapacitance properties, as seen in carbon capacitor studies [16, 17]. The largest proportion of the current is due to double layer charging of the carbon film, with two superposed faradaic contributions in some curves consisting of a reversible signal at 0.55 V-0.6 V, that can be ascribed to reactivity of the metallic substrate corrosion products confined in the pores of the carbon layer, and a steep increase in current above 1.1 V due to substrate oxidation. The assignation of both faradaic signals was confirmed by voltammetries performed on carbon coatings deposited on a non-corroding carbon substrate, and on a naked stainless steel substrate (Check supplementary material S1 and S2).

The double layer charging current (j_{DL}) can be used to probe the electrochemical area of the porous carbon, which is the area in contact with the electrolyte, according to:

$$j_{DL}=C_{DL}\cdot v\cdot w_C\cdot A_C\cdot S \quad (3)$$

where C_{DL} ($F\cdot m_C^{-2}$) is the specific capacitance of the carbon surface, v ($V\cdot s^{-1}$) the voltage sweep rate, w_C ($g_C\cdot cm^{-2}$) the carbon load, A_C ($cm^2\cdot g_C^{-1}$) the mass specific area of carbon, and S the fraction of carbon surface in contact with water, which is related with the water saturation of the pores volume (S=1 for a flooded layer).

Plots in Fig. 5 reflect an important dependence of j_{DL} with the carbon load. A procedure must be followed to extract j_{DL}, as to from the superposed faradaic signals, as explained in supplementary material S3. The dependences of the double layer current density and the mass specific current (j_{DL}/w_C) on the carbon load (w_C) are plotted in Fig. 6 for electrosprayed and airbrushed carbon films. The electrosprayed films show high current densities at low carbon weights followed by a constant value upon increasing carbon load. For the airbrushed film the double layer current density increases with carbon load, and the mass specific current shows no local maximum as the electrosprayed film. The values before and after hydrophilic treatment are only shown for this latter, since the hydrophilic treatment had no significant effect for electrosprayed layers.

The evolution of j_{DL} in Fig. 6a is determined by the hydrophobicity of the porous carbon layers. The airbrushed films show much larger double layer current densities reflecting their low hydrophobicity; in contrast, the electrosprayed films show low current densities caused due to a reduced number of contact points between the carbon surface and the electrolyte due to the superhydrophobicity of the layers.

The peaks in j_{DL} and j_{DL}/w_C at low carbon load in electrosprayed films should be further commented. It reflects an unexpected penetration of the electrolyte into the porous electrosprayed film between 0.1-0.2 $mg_C \cdot cm^{-2}$, in spite of its superhydrophobicity. This behavior may be caused by the distant interaction of the liquid water from the electrolyte meniscus with the hydrophilic substrate through the macropores of the carbon coating. Such distant interaction is observed between water drops [18], and caused by the vapor atmosphere surrounding the liquid surfaces. Similar effect was observed when a water drop is deposited on a thin hydrophobic Pt/C electrosprayed layer on top of a hydrophilic Nafion membrane, in this case leading to a deformation of the membrane [19]. Fig. 7 shows the distant interaction effect of a water drop above a carbon/Nafion layer deposited on top of a Nafion 212R membrane, where membrane deformation can be observed while the surface deposit maintains its superhydrophobicity (Check video 2 in supplementary material). The distant interaction appears active for hydrophobic layers below 50 μm thickness (cf. Fig. 3); whereas it is suppressed on thicker films so the water meniscus is kept at the top surface of the carbon film and the specific double layer current decreases (cf. Fig. 6a).

Another interesting feature in Fig. 6b is the reduction of the specific current density (j_{DL}/w_C) for high loading airbrushed layers. It could be attributed to the presence of a continuous gradient of electrolyte into the film resulting from a mixture of air-filled and liquid-filled pores for films with contact angles around 100º [6]. A very small increase of current is also observed for high loading electrosprayed coatings, but this trend is probably caused by the enhancement of the surface contact area at the outer part due to the morphological change to larger globular agglomerates.

3.3 Characterization of substrate corrosion

The reversible signal at 0.55-0.60 V in Fig. 5 is attributed to substrate corrosion products entrapped by the porous film according to different experimental facts. The signal is absent during first cycle of the voltammetry, and starts growing on successive cycles up to a steady-state value and its intensity diminishes by decreasing voltage sweep rate as a consequence of products diffusion from the substrate surface; in addition, the signal is absent in voltammetries on naked stainless steel substrates, where corrosion products may diffuse freely (see supplementary material). Full protective behavior of carbon coatings is attained for electrosprayed layers at loads above 0.4 $mg_C \cdot cm^{-2}$, for which the double layer current decreases to a minimum (Fig.6a). For airbrushed films, no protective behavior is attained.

Upon immersion, open circuit potential (OCP) has been measured in oxygen-saturated electrolyte for bare and coated stainless steel substrates (see supplementary material S4). Stabilized values of the OCP are presented in Table 1. The protective character of the carbon layers has been further tested in Fig. 8 by means of chronoamperograms recorded at 1.35 V vs SHE (this potential is appropriate to mimic anode degradation in an accelerated fuel cell test [20]). Unprotected cases show rising current densities upon polarization, which is indicative for the increasing roughness of a corroding substrate, as observed for the naked stainless steel, the airbrushed films, and the electrospray films below 0.17 $mg \cdot cm^{-2}$. Full protection is characterized by lower current values with constant decay, as observed with electrosprayed layers above 0.40 $mg \cdot cm^{-2}$. It must be noticed that the carbon loads required for the protective electrosprayed coatings correspond to those loads in Fig. 6a where the reversible signal in the voltammetric tests is absent (Fig.5). Electrosprayed samples presented no significant changes in the chronoamperometric response even after a week in corrosive media with periodic polarization experiments.

The corrosion and protective behaviors of carbon coatings are observed by optical micrographs of the stainless steel substrate after removing the 0.40 $mg \cdot cm^{-2}$ coatings (Fig. 9). The electrosprayed coated substrate leaves unmodified the substrate surface, whereas the airbrushed layer reflects strong degradation as for a naked substrate. Airbrushed layers failed after chronoamperometric tests, showing zones of preferential corrosion and cracks in the layer, allowing free access for the electrolyte to the surface of the substrate.

Further analysis of corrosion kinetics is carried out from potentiodynamic experiments. Tafel plots obtained for the bare substrate and for airbrushed and electrosprayed coatings with a carbon loading of 0.4 $mg \cdot cm^{-2}$ after chronoamperometric experiments are presented in Fig. 10. Lower current and more positive corrosion potential are the indications of the protective character of the electrosprayed layer compared with the airbrushed layer. Table 1 presents the values of anodic (b_a) and cathodic (b_c) Tafel slopes, corrosion potential (E_{corr}) and corrosion current density (j_{corr}) extracted from Fig. 10. Corrosion current density is also calculated with the Stern-Geary relationship using the polarization resistance (R_p), which is defined as the slope of the polarization curve at the corrosion potential [21]. The values show an increase of the corrosion potential by 0.4 V and a decrease of two orders of magnitude of the corrosion current in electrosprayed coated stainless steel compared to the bare substrate. As a reference for fuel cell application of these layers, the U.S. DOE recommends a bipolar plate corrosion (both anodic and cathodic) below 1 $\mu A \cdot cm^{-2}$ for PEM bipolar plates in its technical targets for 2020 [22], which is sufficiently accomplished with the electrosprayed film. It can be concluded that this type of coating could provide a suitable protective character to stainless steel bipolar plates or metal contacts for PEMFCs.

4. Conclusions

Carbon black layers have been deposited on stainless steel substrates by electrospray. The electrosprayed layers are characterized by macroporous morphology, with a change in morphology from dendritic to globular growth with the coating thickness. Water contact angle measurements evidence their superhydrophobicity. Double layer current dependence on carbon layer thickness shows a change in water penetration in the film that we attribute to the distant interaction of water vapor with the hydrophilic substrate. Their voltammetric response in sulfuric acid solution reflects a complete and stable protective behavior of electrosprayed carbon layers for coatings above 0.4 $mg_C \cdot cm^{-2}$. Layers of identical composition grown with airbrush show the loss of hydrophobicity after 24 h contact with electrolyte solution. As a consequence, they are not able to protect the substrate. Corrosion experiments in sulphuric acid show that the electrospray deposited carbon black composite is appropriate for protecting the surface of metal substrates. Electrosprayed carbon layers are good candidates as coatings for metallic flow field plates and contacts used in low temperature fuel cells.

Acknowledgments

This work is being financed by Ministry of Economy of Spain, under E-LIG-E project (ENE2015 70417-P). The authors acknowledge the help of Nuria Germán with the optical microscope images and also wish to thank Breixo Lousada for the video editing.

Declarations of interest: none

Data availability

The raw/processed data required to reproduce these findings cannot be shared at this time as the data also forms part of an ongoing study.

References

[1] R.A. Antunes, M.C.L. Oliveira, G. Ett, V. Ett, Corrosion of metal bipolar plates for PEM fuel cell: A review, Int. J. Hydrogen Energy 35 (2010) 3632-3647.

[2] H. Husby, O. E. Kongstein, A. Oedegaard, F. Seland, Carbon-polymer composite coatings for PEM fuel cell bipolar plates, Int. J. Hydrogen Energy 39 (2014) 951-957.

[3] L. Ejenstam, M. Tuominen, J. Haapanen, J.M. Mäkelä, J. Pan, A. Swerin, P.M. Claesson, Long-term corrosion protection by a thin nano-composite coating, Appl. Surf. Sci. 357 (2015) 2333-2342.

[4] M.A. Frank, C. Meltzer, B. Braunschweig, W. Peukert, A.R. Boccaccini, S. Virtanen, Functionalization of steel surfaces with organic acids: Influence on wetting and corrosion behavior, Appl. Surf. Sci. 404 (2017) 326-333.

[5] C.L. Xu, Y.Z. Wang, Durability, anti-corrosion and self-clean in air/oil of a transparent superhydrophobic polyimide film, Appl. Mater. Today. 10 (2018) 18-23.

[6] D.A. Doshi, P.B. Shah, S. Singh, E.D. Branson, A.P. Malanoski, E.B. Watkins, J. Majewski, F. van Swol, C.F. Brinker, Investigating the interface of superhydrophobic surfaces in contact with water, Langmuir 21 (2005) 7805-7811.

[7] P.M. Barkhudarov, P.B. Shah, E.B. Watkins, D.A. Doshi, C.F. Brinker, J. Majewski, Corrosion inhibition using superhydrophobic films, Corros. Sci. 50 (2007) 897-902.

[8] A. M. Chaparro, M. A. Folgado, P. Ferreira-Aparicio, A. J. Martín, I. Alonso-Álvarez, L. Daza, Properties of catalyst layers for PEMFC electrodes prepared by electrospray deposition, J. Electrochem. Soc. 157 (2010) B993-B999.

[9] P. Ferreira-Aparicio, A. M. Chaparro, M. A. Folgado, J. J. Conde, E. Brightman, G. Hinds, Degradation study by start-up/shut-down cycling of superhydrophobic electrosprayed catalyst layers using a localized reference electrode technique, ACS Appl. Mater. Interfaces 9 (2017) 10626–10636.

[10] J. J. Conde, A. M. Chaparro, P. Ferreira-Aparicio, Understanding the behavior of electrosprayed carbon black-Nafion composite layers, Fuel Cells, in press.

[11] H. Kahlert, Reference Electrodes, in: F. Scholz (Ed.), Electroanalytical Methods: Guide to Experiments and Applications, Springer-Verlag, Berlin, 2002, pp. 261–278.

[12] W. Wen, K. Lu, Electric-field-induced diffusion-limited aggregation, Phys. Rev. E 55 (1997) R2100-R2103.

[13] G. Wang, S. Liu, S. Wei, Y. Liu, J. Lian, Q. Jiang, Robust superhydrophobic surface on Al substrate with durability, corrosion resistance and ice-phobicity, Sci. Rep. 6 (2016) 20933.

[14] J. Jia, J. Fan, B. Xu, H. Dong, Microstructure and properties of the super-hydrophobic films fabricated on magnesium alloys, J. Alloys Compd. 554 (2013) 142-146.

[15] D. Quéré, Wetting and roughness, Annu. Rev. Mater. Res. 38 (2008) 71-99.

[16] E. Frackowiak, F. Béguin, Carbon materials for the electrochemical storage of energy in capacitors, Carbon 39 (2001) 937-950.

[17] H.A. Andreas, B.E. Conway, Examination of the double-layer capacitance of an high specific-area C-cloth electrode as titrated from acidic to alkaline pHs, Electrochim. Acta 51 (2006) 6510-6520.

[18] N. J. Cira, A. Benusiglio, M. Prakash, Vapour-mediated sensing and motility in two-component droplets, Nature 519 (2015) 446-450.

[19] A.M. Chaparro, P. Ferreira-Aparicio, M.A. Folgado, E. Brightman, G. Hinds, Study of superhydrophobic electrosprayed catalyst layers using a localized reference electrode technique, J. Power Sources 325 (2016) 609–619.

[20] A. Orsi, O.E. Kongstein, P.J. Hamilton, A. Oedegard, I.H. Svenu, K. Cooke, An investigation of the typical corrosion parameters used to test polymer electrolyte fuel cell bipolar plate coatings, with titanium nitride coated stainless steel as a case study, J. Power Sources 285 (2015) 530–537.

[21] U. Angst, M. Büchler, On the applicability of the Stern-Geary relationship to determine instantaneous corrosion rates in macro-cell corrosion, Mater. Corros. 66 (2015) 1017-1028.

[22] DOE Technical Targets for Polymer Electrolyte Membrane Fuel Cell Components. Office of Energy Efficiency & Renewable Energy, U.S. Department of Energy. https://energy.gov/eere/fuelcells/doe-technical-targets-polymer-electrolyte-membrane-fuel-cell-components (accessed 20 January 2018)

Tables

Table 1. Values of open circuit potential, Tafel constants, corrosion potential, corrosion current density and polarization resistance for bare and airbrushed and electrospray coated stainless steel in 0.5M H_2SO_4.

	OCP [1] ***mV vs SHE***	E_{corr} ***mV vs SHE***	b_a ***mV·dec^{-1}***	b_c ***mV·dec^{-1}***	j_{corr} ***(Tafel)*** ***µA·cm^{-2}***	R_p ***kΩ·cm^2***	j_{corr} ***(Stern-Geary)*** ***µA·cm^{-2}***
SS 310S	495	- 44	80	426	6.5	2.8	24.0
Airbrush	590	60	85	423	3.7	8.4	8.3
Electrospray	618	460	300	428	0.1	326.7	0.5

[1] **After stabilization in oxygen saturated electrolyte.**

Figure captions

Fig. 1. SEM images of the surface of carbon black composite layers deposited on stainless-steel substrate by a) electrospray, and b) airbrushing. The carbon coating in both cases is 0.4 $mg_C \cdot cm^{-2}$.

Fig. 2. SEM images of carbon black layers deposited on stainless-steel substrate by electrospray with different carbon loads. ES stands for electrospray and AB for airbrush: 1) 0.17 $mg \cdot cm^{-2}$, 2) 0.40 $mg \cdot cm^{-2}$, 3) 0.8 $mg \cdot cm^{-2}$.

Fig. 3. Thickness of carbon films as a function of carbon load prepared by electrospray and airbrushing.

Fig. 4. Water drop contact angle on carbon films deposited on a stainless steel plate, as a function of the carbon load in the coating. Also indicated the value of the uncovered substrate. Measurements were obtained after hydrophilic stabilization of the films.

Fig. 5. Voltammetries of carbon black on stainless steel substrate deposited by electrospray (a and b) and airbrush (c) at 0.1 $V \cdot s^{-1}$ sweep rate, in H_2SO_4 0.5M deaerated solution, at room temperature (23 ºC).

Fig. 6. Double layer a) charging current density (j_{DL}) and b) mass specific charging current density ($j_{DL} \cdot w_C^{-1}$), for electrosprayed and airbrushed carbon black coatings on stainless steel, as a function of carbon load. Before (dotted) and after (solid) hydrophilic treatment.

Fig. 7. Images of a 0.2 $mg \cdot cm^{-2}$ carbon layer on Nafion 212R substrate with a water drop in its surroundings. The initial state corresponds to a) while b) shows the membrane deformation 60s later.

Fig. 8. Chronoamperograms (1.35 V vs. SHE) of carbon black deposited on stainless steel substrates by electrospray and aerography at different carbon loads. ES stands for electrospray and AB for airbrush.

Fig. 9. Micrographs of the stainless steel substrate: a) before and after chronoamperometric measurements of b) 0.4 $mg \cdot cm^{-2}$ electrospray layer, c) 0.4 $mg \cdot cm^{-2}$ airbrush layer and d) naked stainless steel substrate.

Fig. 10. Tafel plots for uncovered stainless steel and airbrushed and electrosprayed coated substrates with 0.4 $mg \cdot cm^{-2}$ carbon loading in 0.5M H_2SO_4 at 0.001 $V \cdot s^{-1}$.

Supplementary material

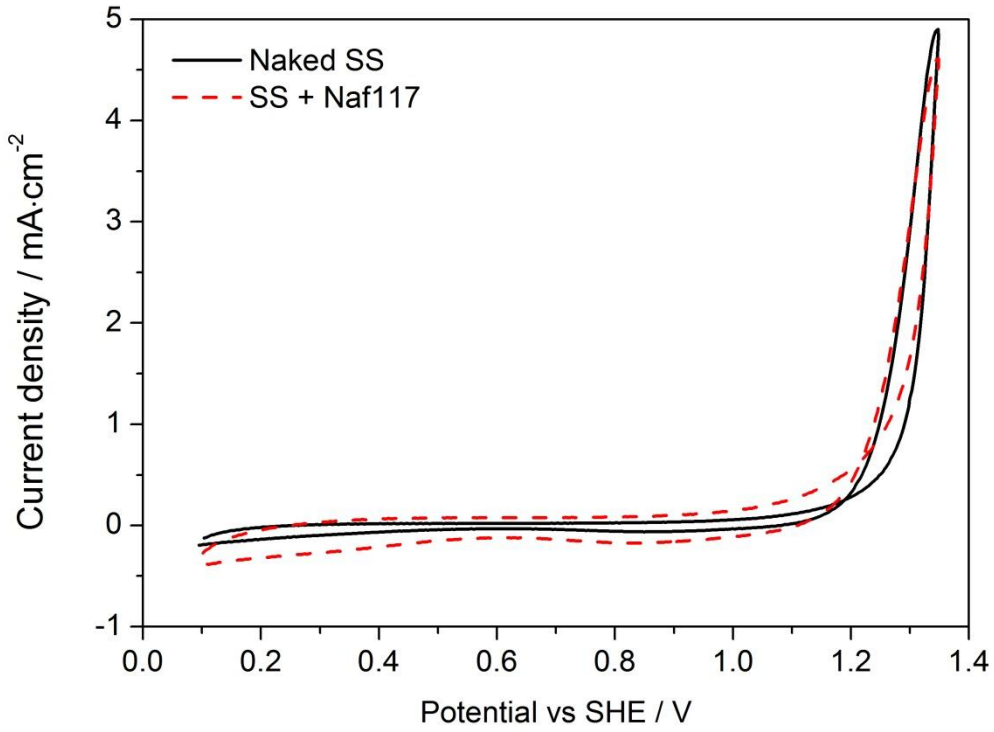

Fig. S1. Cyclic voltammetries of a stainless steel 310S substrate and the same substrate with a membrane of Nafion 117 on top of it. CVs were taken at 0.1 $V \cdot s^{-1}$ in 0.5 M H_2SO_4.

In this figure, the stabilized cyclic voltammetry of a bare SS 310S substrate is presented with that of the same substrate with a Nafion 117 membrane on top of it, to prove that Nafion allows the transport of metallic ions to the electrolyte solution, with a slight decrease of the oxidative current at high potentials and also a slight increase of reduction current, probably due to Nafion diffusion hindrance of the corrosion products.

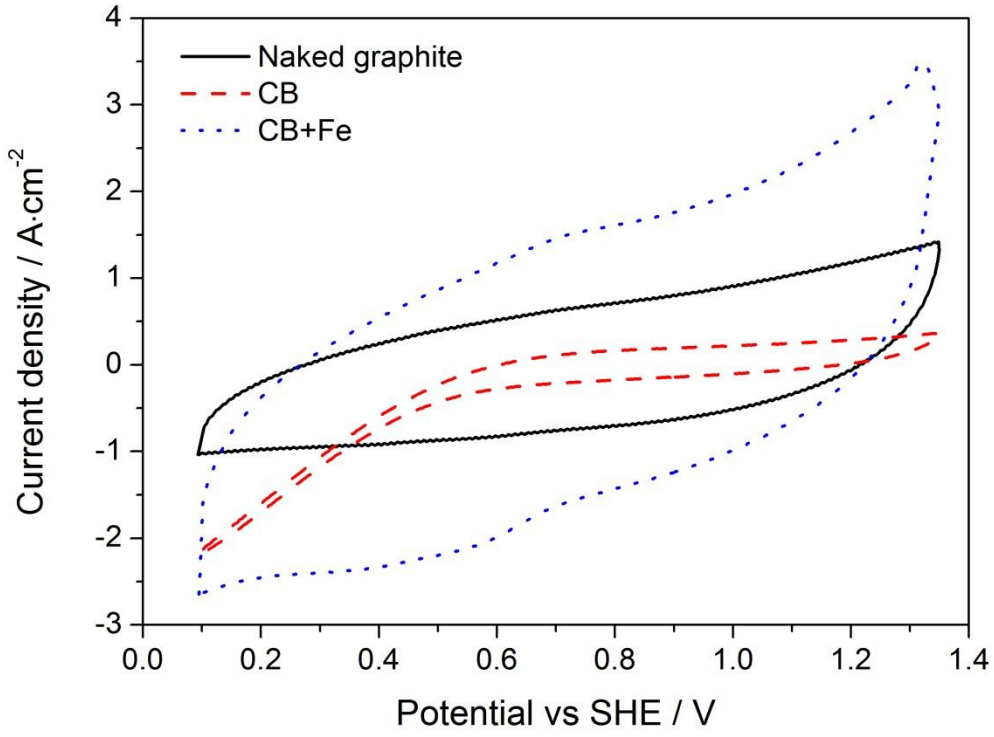

Fig. S2. Cyclic voltammetries of a graphite substrate and 0.4 mg·cm^{-2} electrosprayed layer with and without Fe ions entrapped in Nafion. CVs were taken at 0.1 V·s^{-1} in 0.5 M H_2SO_4.

In order to test that the reversible potential process at 0.55-0.70 V was indeed caused by entrapped Fe ions, a non-metallic substrate (graphite disk) was used to deposit a Nafion film contaminated with Fe^{3+} ions. This is confirmed since the reversible process appears in artificially contaminated Nafion without a Fe ions source in the substrate. The growth of the double layer current is caused by the hydrophilic nature of the Nafion-contaminated layer. The impurity source was iron (III) nitrate nonahydrate previously added to the Nafion 5 wt% solution before the ink preparation.

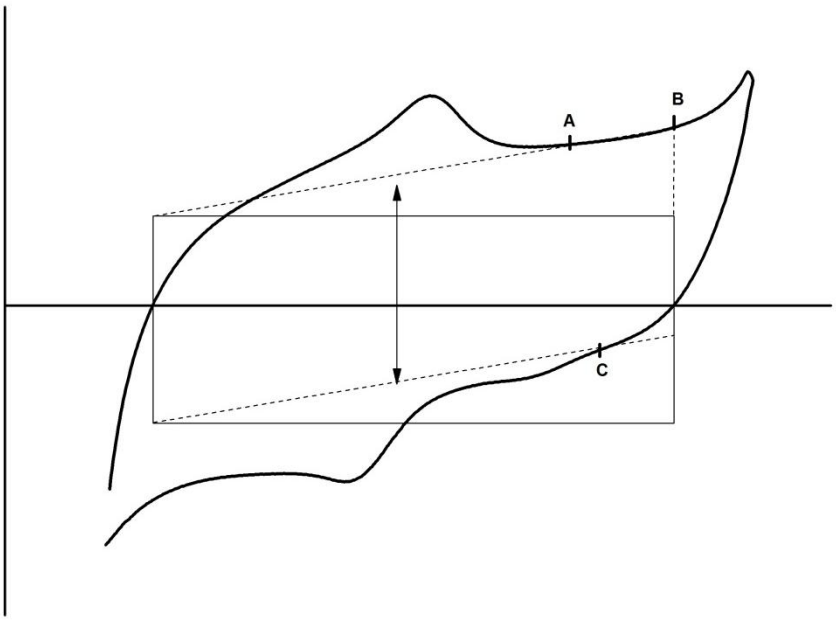

Fig. S3. Schematic of the determination of the double layer in a tilted cyclic voltammetry with superimposed faradaic processes.

Double layer calculation steps:

1- Find a flat zone in the oxidation process with capacity contribution (points A and B)

2- Draw a line between points A and B

3- Find a point C with no contribution of faradaic current

4- Draw a parallel line crossing point C

5- Half of the current value between parallel lines is the double layer current

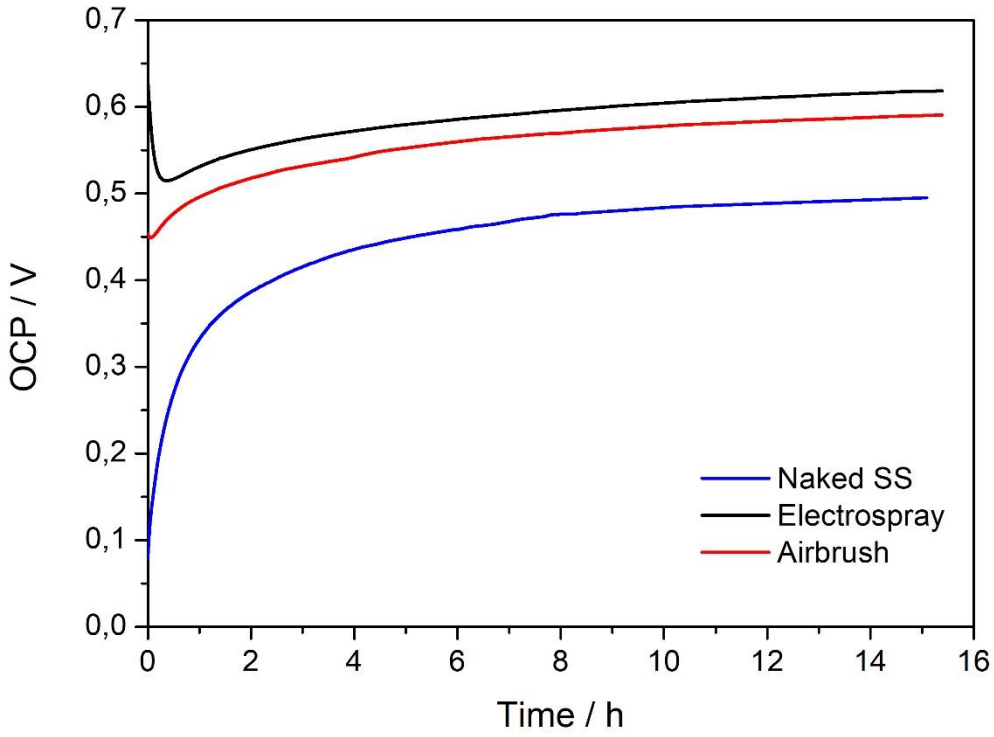

Fig. S4. Open circuit potential (vs. SHE) determination of bare and coated SS310 in oxygen saturated 0.5 M H_2SO_4

OCP was measured with vigorous oxygen bubbling in order to saturate the electrolyte with dissolved oxygen and ensure electrolyte agitation.

Supports were polished and cleaned just before the experiments, so air passivation could be disregarded. Time = 0 corresponds to the immersion of the samples in the electrolyte.